Block Frequency Spreading: A Method for Low-Complexity MIMO in FBMC-OQAM

Ronald Nissel[†], Jiri Blumenstein[‡], and Markus Rupp[†]
[†]Christian Doppler Laboratory for Dependable Wireless Connectivity for the Society in Motion, TU Wien, Vienna, Austria
[‡]The Faculty of Electrical Engineering and Communication, Brno University of Technology, Brno, Czech Republic
Email: rnissel@nt.tuwien.ac.at, blumenstein@feec.vutbr.cz, mrupp@nt.tuwien.ac.at

***Abstract*—Filter Bank Multi-Carrier (FBMC) offers better spectral properties than conventional Orthogonal Frequency Division Multiplexing (OFDM). However, the lack of Multiple-Input and Multiple-Output (MIMO) compatibility is one of its biggest obstacles. By spreading symbols in frequency, we are able to restore complex orthogonality in FBMC, so that all MIMO methods known in OFDM can be straightforwardly applied. The spreading process itself has low computational complexity because it is based on a Fast-Walsh-Hadamard transform, thus completely free of multiplications. Orthogonality only holds if the channel is approximately frequency flat within the spreading length. We thus suggest the usage of frequency blocks which are separated by a guard subcarrier. We also investigate the effect of a doubly selective channel on our block frequency spreading approach. Finally, MIMO simulations validate the applicability.**

***Index Terms*—FBMC-OQAM, MIMO, Walsh-Hadamard Coding, Multipath channels, Time-varying channels.**

I. Introduction

Filter Bank Multi-Carrier (FBMC) with Offset Quadrature Amplitude Modulation (OQAM), in short just FBMC, has better spectral properties compared to Orthogonal Frequency Division Multiplexing (OFDM) and usually does not need a Cyclic Prefix (CP) [1]. All this nice features of FBMC, however, come at a price, namely, an intrinsic imaginary interference. A theoretical explanation for the imaginary interference can be found in the Balian-Low theorem. In many cases, the imaginary interference has either no, or only a minor influence on the performance. However, some important techniques, such as pilot symbol aided channel estimation [2], Alamouti's space-time-block-code [3] or maximum likelihood Multiple-Input and Multiple-Output (MIMO) detection [4] are seriously hampered by the imaginary interference and innovative solutions for those challenges need to be found. While there exist many practical solutions for channel estimation [5], the issue of MIMO transmissions is not fully solved yet. The intrinsic imaginary interference prevents a straightforward implementation of space time block codes such as Alamouti's. However, by considering not only one data symbol, but rather clustered symbols, we can circumvent the Balian-Low theorem and restore complex orthogonality. In [3], a Hadamard spreading approach was proposed to enable Alamouti space-time-block-code. Similar, [4] suggested Fast Fourier Transform (FFT) spreading in time. On the other hand, authors in [6] proposed a block-Alamouti scheme (over time). The same method was recently applied by [7] in the frequency domain. In this paper, we follow the Hadamard spreading approach suggested in [3]. Compared to the recently introduced method in [7], our approach has the following advantages: Firstly, we restore complex orthogonality. Thus, our method not only works for 2×1 Alamouti (as in [7]), but additionally allows to straightforwardly use all other methods known in OFDM, such as channel estimation, space-time-block codes for a higher number of antennas or low-complexity maximum likelihood symbol detection. Secondly, the peak-to-average power ratio is slightly lower due to the spreading process. Thirdly, compared to [7], the required guard overhead is reduced by a factor of two. The disadvantages, on the other hand, are: Firstly, a slightly higher computational complexity. However, only summations are required; no multiplications are necessary! Additionally, by employing a Fast-Walsh-Hadamard transform, we can further decrease the computational complexity, so that it becomes almost neglectable. Secondly, the spreading length must be a power of two. By comparing the pros and cons of our method with the technique proposed in [7], it is evident that Hadamard spreading provides the overall better package.

The novel contribution of our paper can be summarized as follows:

- Authors in [3] assume a frequency flat channel for the frequency spreading approach. We, on the other hand, allow for a doubly-selective channel, propose a block frequency spreading approach and derive closed-form expressions for the induced signal-to-interference ratio.
- In contrast to our paper in [8], [9], we spread in frequency instead of time. This reduces the latency and improves the robustness in a time-variant channel.

In order to support reproducibility, our MATLAB code can be downloaded at **https://www.nt.tuwien.ac.at/downloads/**.

II. FBMC-OQAM

In FBMC we transmit symbols over a rectangular time-frequency grid. Let us denote the transmit symbol at subcarrier position l and time-position k by $x_{l,k}$. The transmitted signal, consisting of L subcarriers and K time-symbols, can then be expressed as:

$$s(t) = \sum_{k=1}^{K} \sum_{l=1}^{L} g_{l,k}(t)\, x_{l,k}, \tag{1}$$

978-1-5090-3009-5/17/$31.00

with

$$g_{l,k}(t) = p(t - kT)\, \mathrm{e}^{\mathrm{j}2\pi\, lF\,(t-kT)}\, \mathrm{e}^{\mathrm{j}\frac{\pi}{2}(l+k)}. \tag{2}$$

The basis pulse $g_{l,k}(t)$ is, essentially, a time and frequency shifted versions of the prototype filter $p(t)$. We employ the PHYDYAS prototype filter [10]. The variable T denotes the time-spacing and F the frequency spacing (subcarrier spacing). In FBMC, the prototype filter $p(t)$ is orthogonal for a time-frequency spacing of $TF = 2$. To achieve the same data rate as in OFDM (without CP), we reduce the time-spacing as well as the frequency spacing by a factor of two, leading to $TF = 0.5$. This time-frequency squeezing causes interference, which, however, is shifted to the purely imaginary domain by the phase shift $\mathrm{e}^{\mathrm{j}\frac{\pi}{2}(l+k)}$. Taking the real part removes the imaginary interference and allows low-complexity symbol detection. However, we can only transmit real-valued symbols $x_{l,k} \in \mathbb{R}$ in such a way. The underlying imaginary interference in FBMC is problematic for some MIMO techniques, which justifies the block frequency approach presented in Section III.

To simplify analytical investigations, we consider a discrete-time representation in combination with a vector notation [1]. The sampled transmit signal $\mathbf{s} \in \mathbb{C}^{N\times 1}$, see (1), can then be expressed by:

$$\mathbf{s} = \mathbf{G}\,\mathbf{x}, \tag{3}$$

with

$$\mathbf{G} = \begin{bmatrix} \mathbf{g}_{1,1} & \mathbf{g}_{2,1} & \cdots & \mathbf{g}_{L,1} & \mathbf{g}_{1,2} & \cdots & \mathbf{g}_{L,K} \end{bmatrix}. \tag{4}$$

Transmit matrix $\mathbf{G}$ is build-up by the transmit vector $\mathbf{g}_{l,k} \in \mathbb{C}^{N\times 1}$, representing the sampled basis pulse in (2). On the other hand, transmit symbol vector $\mathbf{x} \in \mathbb{C}^{LK\times 1}$ in (3) is defined as:

$$\mathbf{x} = \mathrm{vec}\left\{ \begin{bmatrix} x_{1,1} & \cdots & x_{1,K} \\ \vdots & \ddots & \vdots \\ x_{L,1} & \cdots & x_{L,K} \end{bmatrix} \right\} \tag{5}$$

$$= \begin{bmatrix} x_{1,1} & x_{2,1} & \cdots & x_{L,1} & x_{1,2} & \cdots & x_{L,K} \end{bmatrix}^{\mathsf{T}}. \tag{6}$$

In an Additive White Gaussian Noise (AWGN) channel, a matched filter maximizes the Signal-to-Noise Ratio (SNR), so that the receive matrix is chosen as $\mathbf{G}^{\mathsf{H}}$. The whole transmission system can then be expressed by:

$$\mathbf{y} = \mathbf{G}^{\mathsf{H}}\mathbf{G}\,\mathbf{x} + \mathbf{G}^{\mathsf{H}}\mathbf{n}, \tag{7}$$

where $\mathbf{n}$ represent the Gaussian noise, $\mathbf{n} \sim \mathcal{CN}(\mathbf{0}, P_{\mathrm{n}}\,\mathbf{I}_N)$. The real orthogonality condition in FBMC implies that the transmission matrix is orthogonal only in the real domain, that is, $\Re\{\mathbf{G}^{\mathsf{H}}\mathbf{G}\} = \mathbf{I}_{LK}$. In the appendix, we provide a simple example for such transmission matrix. As comparison, OFDM has (complex) orthogonality, $\mathbf{G}^{\mathsf{H}}\mathbf{G} = \mathbf{I}_{LK}$. Note that for the same transmission bandwidth FL and the same transmission time KT, both systems have the same bit rate (OFDM without CP), despite the fact that FBMC only transmits real-valued symbols ($\rightarrow$ half the information). This is possible because FBMC transmits twice as many symbols within the same time interval.

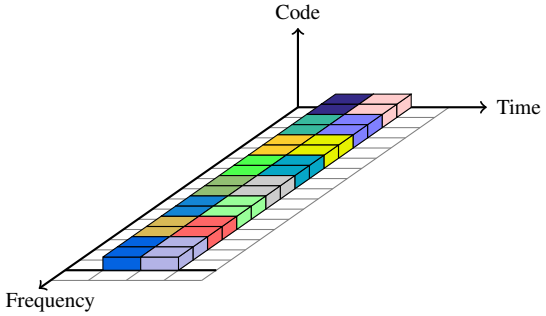

Fig. 1. In conventional FBMC-OQAM, real valued symbols are transmitted over a rectangular time-frequency grid ($TF = 0.5$). Two real valued symbols are required to transmit one complex valued symbol. Thus, the name "offset"-QAM whereas we apply the offset not in time (as often done in literature) but in frequency to be consistent with Fig. 2. Illustration: $L = 16$, $K = 2$.

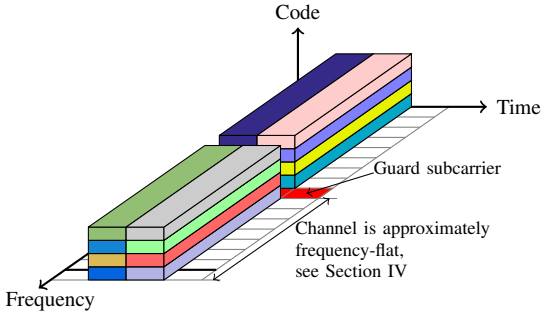

Fig. 2. In coded FBMC-OQAM, complex valued symbols are spread over several subcarriers. The spreading process itself has negligible computational complexity because a Fast-Walsh-Hadamard transform can be used. Different frequency blocks are separated by a guard subcarrier. Fig.: $L = 8$, $K = 2$ and two frequency blocks $\rightarrow$ same number of data symbols as in Fig. 1.

III. Block Frequency Spreading

Fig. 1 illustrates a conventional FBMC transmission. As explained in Section II, we can only transmit real-valued data symbols in FBMC due to the imaginary interference, limiting the applicability of certain techniques such as Alamouti's space time block codes. By spreading symbols in frequency, however, we are able to restore complex orthogonality, so that all transmission techniques known in OFDM, such as Alamouti's space time block codes or multi-user precoding, can be straightforwardly applied in FBMC (on a frequency-block basis instead of per-subcarrier). Our block frequency spreading approach is illustrated in Fig. 2. We assume that the channel is approximately frequency-flat within the spreading interval and approximately time-flat for the duration of one FBMC symbol. This allows the employment of low-complexity equalizers and enables the straightforward usage of MIMO. In Section IV, we will explain in more detail what "approximately" frequency-flat and "approximately" time-invariant means. As indicated in Fig. 2, we add a guard subcarrier between blocks to mitigate interference (orthogonality is only restored within the same block). Because the PHYDYAS prototype filter has very sharp edges in the frequency domain, those frequency blocks are completely separated. This is different to the time-spreading approach we presented in [8], where block interference occurs due to the underlying Hermite prototype filter. A minor

drawback of the guard subcarrier is a reduction in the time-frequency efficiency. We define the time-frequency efficiency loss by

$$\eta = \frac{1}{L+1}. \tag{8}$$

For example, if we spread over $L = 32$ subcarriers, $\eta = 3\%$, implying that the data rate of our approach is 3% lower compared to conventional FBMC. However, a 1.4 MHz Long Term Evolution (LTE) system has an efficiency loss of 28% (72 out of 93.33 subcarriers and a CP length of 4.7μs), so that the efficiency loss of our block frequency spreading approach is relatively low (and to some extend scalable).

Let us now mathematically describe the spreading approach. At the transmitter, we spread the data symbols $\tilde{\mathbf{x}} \in \mathbb{C}^{\frac{LK}{2}\times 1}$ by a precoding (spreading) matrix $\mathbf{C} \in \mathbb{R}^{LK\times\frac{LK}{2}}$, according to

$$\mathbf{x} = \mathbf{C}\,\tilde{\mathbf{x}}. \tag{9}$$

At the receiver, we de-spread the received symbols by $\mathbf{C}^{\mathsf{H}}$, so that the received data symbols $\tilde{\mathbf{y}} \in \mathbb{C}^{\frac{LK}{2}\times 1}$ can be written as:

$$\tilde{\mathbf{y}} = \mathbf{C}^{\mathsf{H}}\,\mathbf{y}. \tag{10}$$

Orthogonality is restored if we are able to find a coding matrix $\mathbf{C}$ which satisfies the following orthogonality condition,

$$\mathbf{C}^{\mathsf{H}}\mathbf{G}^{\mathsf{H}}\mathbf{G}\mathbf{C} = \mathbf{I}_{LK/2}, \tag{11}$$

where $\mathbf{G}^{\mathsf{H}}\mathbf{G}$ represents the FBMC transmission matrix, see (7). By utilizing the underlying structure of our notation (vectorization, see (5) and (6)) and the fact that we spread over frequency only, we are able to rewrite the coding matrix $\mathbf{C}$ by:

$$\mathbf{C} = \mathbf{I}_K \otimes \mathbf{C}_0, \tag{12}$$

where $\mathbf{C}_0 \in \mathbb{R}^{L\times\frac{L}{2}}$ describes the frequency spreading matrix for one time-slot. The Kronecker product $\otimes$ together with the identity matrix then map coding matrix $\mathbf{C}_0$ to the correct time-slot. Finally, we find the coding matrix $\mathbf{C}_0$ by taking every second column out of a sequency ordered [11] Walsh-Hadamard matrix $\boldsymbol{\mathcal{H}} \in \mathbb{R}^{L\times L}$, that is,

$$[\mathbf{C}_0]_{l,m} = [\boldsymbol{\mathcal{H}}]_{l,2m} \quad \text{for} \quad l = 1\dots L;\, m = 1\dots\frac{L}{2}. \tag{13}$$

In the appendix, we provide a simple example of such coding matrix. Note that we could also start from the second column of the Walsh-Hadamard matrix, that is, $[\boldsymbol{\mathcal{H}}]_{l,1+2m}$. In (9) and (10), we describe the spreading process by a coding matrix $\mathbf{C}$. However, we have keep in mind that the internal structure is based on a Walsh-Hadamard matrix, so that a Fast-Walsh-Hadamard transform can be used to reduce the computational complexity. Thus, for each complex valued data symbol, we only need $\log_2(L)-1$ extra additions/subtractions at the transmitter and $\log_2(L)$ extra additions/subtractions at the receiver. No additional multiplications are required! The only minor drawback of the Walsh-Hadamard approach is that the spreading length has to be a power of two.

IV. Doubly-Selective Channels

Wireless channels are characterized by time-variant multi-path propagation, which destroys orthogonality of our system. This results in a certain Signal-to-Interference Ratio (SIR). However, as long as the SIR is approximately 10 dB higher than the SNR, the noise completely dominates the interference which can thus be neglected. Even if the SNR approaches the SIR, we only observe a small performance degeneration equivalent to an SNR shift of approximately 3 dB.

To characterize the influence of a doubly-selective channel, we ignore noise and include a time-variant convolution matrix $\mathbf{H} \in \mathbb{C}^{N\times N}$ in our system, so that (10) together with (7) and (9) transform to:

$$\tilde{\mathbf{y}} = \mathbf{C}^{\mathsf{H}}\mathbf{G}^{\mathsf{H}}\mathbf{H}\mathbf{G}\mathbf{C}\,\tilde{\mathbf{x}}. \tag{14}$$

In a doubly-flat Rayleigh channel, that is, $\mathbf{H} = \bar{h}\,\mathbf{I}_N$ with $\bar{h} \sim \mathcal{CN}(0,1)$, orthogonality still holds. However, in a doubly-selective channel, matrix $\mathbf{H}$ is no longer a scaled identity matrix, leading to off-diagonal elements in $\mathbf{C}^{\mathsf{H}}\mathbf{G}^{\mathsf{H}}\mathbf{H}\mathbf{G}\mathbf{C}$ and thus interference. The diagonal elements, on the other hand, describe the desired signal components and are utilized in a one-tap equalizer. To derive an analytical SIR expression, we consider the received data symbol at code position m and time-position k, so that (14) transforms to:

$$\tilde{y}_{m,k} = \mathbf{c}_{m,k}^{\mathsf{H}}\mathbf{G}^{\mathsf{H}}\mathbf{H}\mathbf{G}\mathbf{C}\,\tilde{\mathbf{x}} \tag{15}$$

$$= \left((\mathbf{G}\mathbf{C}\,\tilde{\mathbf{x}})^{\mathsf{T}} \otimes (\mathbf{c}_{m,k}^{\mathsf{H}}\mathbf{G}^{\mathsf{H}})\right)\mathrm{vec}\{\mathbf{H}\}. \tag{16}$$

Vector $\mathbf{c}_{m,k} \in \mathbb{R}^{N\times 1}$ represents the i-th column of $\mathbf{C}$ with $i = \frac{L}{2}(k-1)+m$. Furthermore, we rewrite (15) by (16) in order to simplify statistical investigations, allowing us to express the SIR by

$$\mathrm{SIR}_{m,k} = \frac{[\boldsymbol{\Gamma}]_{i,i}}{\mathrm{tr}\{\boldsymbol{\Gamma}\} - [\boldsymbol{\Gamma}]_{i,i}}, \tag{17}$$

with $i = \frac{L}{2}(k-1)+m$, and

$$\boldsymbol{\Gamma} = \left((\mathbf{G}\mathbf{C})^{\mathsf{T}} \otimes (\mathbf{c}_{m,k}^{\mathsf{H}}\mathbf{G}^{\mathsf{H}})\right)\mathbf{R}_{\mathrm{vec}\{\mathbf{H}\}}\left((\mathbf{G}\mathbf{C})^{\mathsf{T}} \otimes (\mathbf{c}_{m,k}^{\mathsf{H}}\mathbf{G}^{\mathsf{H}})\right)^{\mathsf{H}}. \tag{18}$$

The j-th diagonal element of $\boldsymbol{\Gamma}$ is denoted by $[\boldsymbol{\Gamma}]_{j,j}$ and represents the contribution of transmit symbol $[\tilde{\mathbf{x}}]_j$ on the received power $\mathbb{E}\{|\tilde{y}_{m,k}|^2\}$. Thus, we can directly calculate the SIR as shown in (17). The statistical properties of the channel are included in the correlation matrix, $\mathbf{R}_{\mathrm{vec}\{\mathbf{H}\}} = \mathbb{E}\{\mathrm{vec}\{\mathbf{H}\}\mathrm{vec}\{\mathbf{H}\}^{\mathsf{H}}\}$, and depend on the power delay profile and the Doppler spectral density.

One of the biggest challenges is to find a meaningful channel model. For example, it has been shown in [12] through real world 3G measurements that in many cases, the Root Mean Square (RMS) delay spread is lower than typically assumed in simulations. We expect that the RMS delay spread will further decrease due to beamforming, higher carrier frequencies and smaller cell sizes. This is particularly important for our frequency spreading approach which only works for a low delay spread. To cover a large range of possible scenarios, we include three different Rayleigh fading

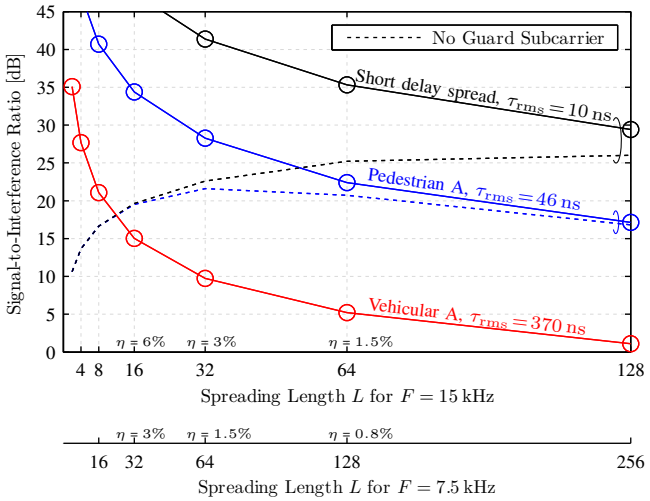

Fig. 3. The interference can be neglected if the SIR is approximately 10 dB higher than the SNR. A guard subcarrier increases the SIR significantly, especially for a short spreading length. The higher the spreading length, the higher the spectral efficiency. However, a high spreading length also leads to high interference caused by the channel.

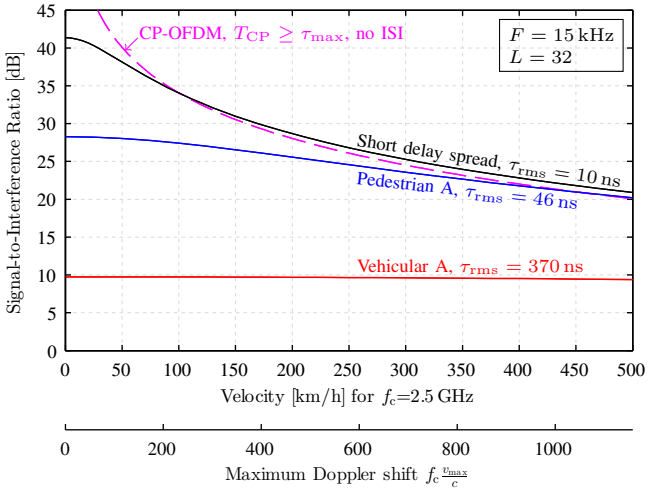

Fig. 4. A time-variant channel leads to additional interference. For high velocities, FBMC shows approximately the same SIR as OFDM. Thus, OFDM no longer performs better in terms of SIR but has a worse spectral efficiency than FBMC. The SIR for velocity zero can be found in Fig. 3.

channel models in our performance evaluation. Firstly the Vehicular A channel model [13] with a relatively large delay spread of 370 ns. Secondly, the Pedestrian A channel model [13] with a moderate delay spread of 46 ns. Thirdly, a short delay spread of 10 ns for which we assume 3 equally spaced taps. These taps are 100 ns apart and the power of each tap is 20 dB lower then the previous tap. Such short delay spread represents, for example, an indoor scenario.

Fig. 3 shows how the SIR, see (17), depends on the spreading length. In many practical cases, the SNR is below 20 dB. Thus, for a short delay spread (10 ns), we can easily spread over $L = 128$ subcarriers, leading to an almost negligible time-frequency efficiency loss of $\eta = 0.8\%$. For a Pedestrian A channel model we are able to spread over $L = 32$ subcarriers, leading to $\eta = 3\%$. Only for a high delay spread, our method is suboptimal due to the large overhead required for a sufficiently high SIR. Alternatively, we could employ multi-tap equalizers at the cost of increased computational complexity [14]. As a reference, we also include the SIR in case of no guard subcarriers (dotted line). In some cases, especially for low to medium SNR ranges, we do not need a guard subcarrier, leading to a maximum spectral efficiency ($\eta = 0\%$).

Fig. 4 shows how the SIR depends on the velocity. Even high velocities, such as 200 km/h, generate only small additional interference, so that the SIR remains sufficiently high for a short delay spread and a Pedestrian A channel model. Compared to the time-spreading approach we investigated in [8], frequency spreading provides higher robustness in time-variant channels. As a reference, we also include the SIR for conventional CP-OFDM.

V. MIMO Simulations

So far, we have presented a detailed description of how spreading can be used to restore complex orthogonality. This allows the straightforward usage of all MIMO techniques known in OFDM. In this section, we validate the applicability of our block frequency spreading approach by simulations. We assume a Pedestrian A channel model and a Jakes Doppler spectrum (velocity 100 km/h at 2.5 GHz). The subcarrier spacing is set to $F = 15$ kHz and the symbol alphabet is chosen from a 16-Quadrature Amplitude Modulation (QAM) signal constellation. For FBMC we assume a spreading length of $L = 32$ and a total of $N_{\mathrm{B}} = 16$ frequency blocks. This leads to a transmission bandwidth of $F(L+1)N_{\mathrm{B}} = 7.92$ MHz. OFDM uses the same bandwidth, that is 528 subcarriers. Note, however, that in practice, OFDM requires additional guards band due to its large out-of-band emissions. The transmission time is for both methods the same and given by $KT = 1$ ms. The zero guard subcarrier in FBMC leads to a slightly higher SNR compared to OFDM (but only by $(L+1)/L = 1.03$ which has almost no influence).

Similar as in [8], we consider 2×1 Alamouti's block coding. Furthermore, we include maximum likelihood symbol detection whereas we ignore any channel induced interference to keep the complexity low. Both of these schemes do not work with conventional FBMC. As a reference, we also include zero forcing equalization.

Fig. 5 shows that FBMC has almost the same Bit Error Ratio (BER) performance as OFDM [15]. FBMC, however, has the additional advantage of much better spectral properties. Only for high SNR values we observe small deviations between OFDM and FBMC. This can be explained by the channel induced interference which leads to an SIR of approximately 27 dB, see Fig. 4. Such interference, however, has no influence for low to medium SNR values. Only for high SNR values, we might have to decrease the spreading length in order to gain robustness.

VI. Conclusion

If the channel delay spread is not too high, block frequency spreading becomes an efficient method to restore complex

$$\mathbf{G^H G} = \begin{bmatrix} 1 & +\text{j}0.2181 & 0 & 0 & +\text{j}0.5769 & +\text{j}0.1912 & 0 & 0 \\ -\text{j}0.2181 & 1 & +\text{j}0.2181 & 0 & -\text{j}0.1912 & -\text{j}0.5769 & -\text{j}0.1912 & 0 \\ 0 & -\text{j}0.2181 & 1 & +\text{j}0.2181 & 0 & +\text{j}0.1912 & +\text{j}0.5769 & +\text{j}0.1912 \\ 0 & 0 & -\text{j}0.2181 & 1 & 0 & 0 & -\text{j}0.1912 & -\text{j}0.5769 \\ -\text{j}0.5769 & +\text{j}0.1912 & 0 & 0 & 1 & +\text{j}0.2181 & 0 & 0 \\ -\text{j}0.1912 & +\text{j}0.5769 & -\text{j}0.1912 & 0 & -\text{j}0.2181 & 1 & +\text{j}0.2181 & 0 \\ 0 & +\text{j}0.1912 & -\text{j}0.5769 & +\text{j}0.1912 & 0 & -\text{j}0.2181 & 1 & +\text{j}0.2181 \\ 0 & 0 & -\text{j}0.1912 & +\text{j}0.5769 & 0 & 0 & -\text{j}0.2181 & 1 \end{bmatrix} \tag{19}$$

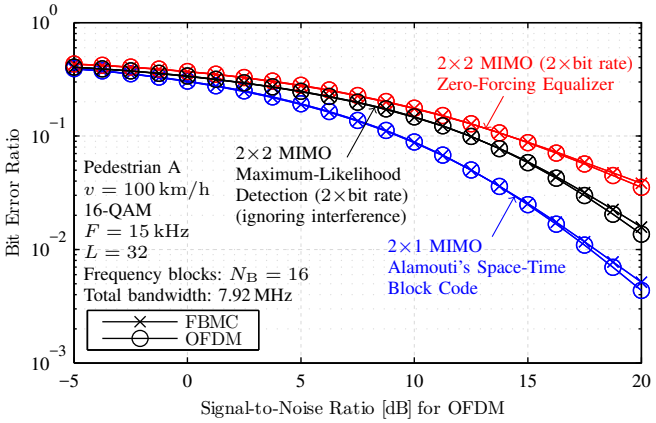

Fig. 5. Simulations validate that FBMC, based on block frequency spreading, has approximately the same BER as OFDM. However, FBMC has the additional advantage of a higher spectral efficiency. Only for high SNR values, we observe small deviations due to channel induced interference, see Fig. 4.

orthogonality in FBMC, allowing us to straightforwardly apply all MIMO methods known in OFDM. To reduce interference between frequency blocks, we might need a guard subcarrier. This reduces the spectral efficiency slightly. The overall spectral efficiency, however, is still much better than in OFDM due to lower out-of-band emissions in FBMC.

Appendix

For a better understanding of our notation and the underlying concept, we provide a simple example for $L = 4$ subcarriers and $K = 2$ FBMC symbols. The transmission matrix in (7) can then be calculated as in (19). Note that only real orthogonality holds true, $\Re\{\mathbf{G^H G}\} = \mathbf{I}_{LK}$. Furthermore, the imaginary interference weight between neighboring subcarriers is given by j0.2181 while between neighboring symbols it is j0.5769. This emphasizes the fact that the PHYDYAS prototype filter has better localization in frequency than in time. By applying the algorithm presented in Section III, see (12) and (13), we find the precoding matrix as:

$$\mathbf{C} = \frac{1}{2} \begin{bmatrix} 1 & 1 & 1 & 1 & 0 & 0 & 0 & 0 \\ 1 & -1 & -1 & 1 & 0 & 0 & 0 & 0 \\ 0 & 0 & 0 & 0 & 1 & 1 & 1 & 1 \\ 0 & 0 & 0 & 0 & 1 & -1 & -1 & 1 \end{bmatrix}^{\mathsf{T}} \tag{20}$$

It can be easily checked that the complex orthogonality condition holds, that is, $\mathbf{C^H G^H G C} = \mathbf{I}_{\frac{LK}{2}}$.

Acknowledgment

The financial support by the Austrian Federal Ministry of Science, Research and Economy, the National Foundation for Research, Technology and Development, and the TU Wien is gratefully acknowledged. The research has been co-financed by the Czech Science Foundation, Project No. 17-18675S "Future transceiver techniques for the society in motion," and by the Czech Ministry of Education in the frame of the National Sustainability Program under grant LO1401.

References

[1] R. Nissel, S. Schwarz, and M. Rupp, "Filter bank multicarrier modulation schemes for future mobile communications," *IEEE Journal on Selected Areas in Communications*, 2017, to appear.

[2] R. Nissel and M. Rupp, "On pilot-symbol aided channel estimation in FBMC-OQAM," in *IEEE International Conference on Acoustics, Speech and Signal Processing (ICASSP)*, Shanghai, China, March 2016.

[3] C. Lélé, P. Siohan, and R. Legouable, "The Alamouti scheme with CDMA-OFDM/OQAM," *EURASIP Journal on Advances in Signal Processing*, vol. 2010, no. 1, p. 1, 2010.

[4] R. Zakaria and D. Le Ruyet, "A novel filter-bank multicarrier scheme to mitigate the intrinsic interference: application to MIMO systems," *IEEE Trans. Wireless Commun*, vol. 11, no. 3, pp. 1112–1123, 2012.

[5] R. Nissel, S. Caban, and M. Rupp, "Experimental evaluation of FBMC-OQAM channel estimation based on multiple auxiliary symbols," in *IEEE Sensor Array and Multichannel Signal Processing Workshop (SAM)*, Rio de Janeiro, Brazil, July 2016.

[6] M. Renfors, T. Ihalainen, and T. H. Stitz, "A block-Alamouti scheme for filter bank based multicarrier transmission," in *European Wireless Conference (EW)*, 2010.

[7] D. Na and K. Choi, "Intrinsic ICI-free Alamouti coded FBMC," *IEEE Communications Letters*, vol. 20, no. 10, pp. 1971–1974, 2016.

[8] R. Nissel and M. Rupp, "Enabling low-complexity MIMO in FBMC-OQAM," in *IEEE Globecom Workshops (GC Wkshps)*, Washington, USA, Dec 2016.

[9] R. Nissel, E. Zöchmann, M. Lerch, S. Caban, and M. Rupp, "Low-latency MISO FBMC-OQAM: It works for millimeter waves!" in *IEEE International Microwave Symposium*, Honolulu, Hawaii, June 2017.

[10] M. Bellanger, D. Le Ruyet, D. Roviras, M. Terré, J. Nossek, L. Baltar, Q. Bai, D. Waldhauser, M. Renfors, T. Ihalainen *et al.*, "FBMC physical layer: a primer," *PHYDYAS, January*, 2010.

[11] J. Manz, "A sequency-ordered fast Walsh transform," *IEEE Transactions on Audio and Electroacoustics*, vol. 20, no. 3, pp. 204–205, 1972.

[12] H. Asplund, K. Larsson, and P. Okvist, "How typical is the "typical urban" channel model?" in *IEEE Vehicular Technology Conference (VTC)*, 2008.

[13] "Recommendation ITU-R M.1225: Guidelines for Evaluation of Radio Transmission Technologies for IMT-2000," ITU, Tech. Rep., 1997.

[14] R. Nissel, M. Rupp, and R. Marsalek, "FBMC-OQAM in doubly-selective channels: A new perspective on MMSE equalization," in *IEEE International Workshop on Signal Processing Advances in Wireless Communications (SPAWC)*, Sapporo, Japan, Jul. 2017.

[15] R. Nissel and M. Rupp, "OFDM and FBMC-OQAM in doubly-selective channels: Calculating the bit error probability," *IEEE Communications Letters*, 2017, to appear.